A high-speed photoconductive UV detector based on an $Mg_{0.4}Zn_{0.6}O$ thin film

2007 Semicond. Sci. Technol. 22 687

(http://iopscience.iop.org/0268-1242/22/7/001)

Semicond. Sci. Technol. **22** (2007) 687–690 doi:10.1088/0268-1242/22/7/001

A high-speed photoconductive UV detector based on an $Mg_{0.4}Zn_{0.6}O$ thin film

D Y Jiang, J Y Zhang, K W Liu, Y M Zhao, C X Cong, Y M Lu, B Yao, Z Z Zhang and D Z Shen

Key Laboratory of Excited State Processes, Changchun Insititute of Optics, Fine Mechanics and Physics, Chinese Academy of Sciences, 16-Dongnanhu Road, Changchun, 130033, People's Republic of China

Received 6 February 2007, in final form 19 April 2007
Published 22 May 2007
Online at stacks.iop.org/SST/22/687

Abstract

A high quality $Mg_xZn_{1-x}O$ thin film with up to ~40 at% Mg incorporation was grown on a quartz substrate by the rf magnetron sputtering technique. The photoconductive type of $Mg_{0.4}Zn_{0.6}O$ metal–semiconductor–metal ultraviolet detector was prepared. The ratio of the ultraviolet to visible was more than four orders of magnitude; the 10%–90% rise and fall times were 16 ns and 250 ns, respectively. Furthermore, the dark current was below 40 nA under 3 V bias and the gain was observed which caused the high responsivity (~1.3 A W^{-1}) at 320 nm, and the corresponding detectivity D^* was 1.37×10^{11} cm $Hz^{1/2}$ W^{-1}. A high-speed response was attributed to the high quality of the $Mg_{0.4}Zn_{0.6}O$ thin film, which was found to dramatically enhance the UV detection properties of the device. The effect of the gain on the fall time and responsivity was analysed in the present work.

1. Introduction

ZnO, a wide band gap ($E_g = 3.37$ eV) semiconductor, is well known as one of the most promising materials for the application of an ultraviolet (UV) detector [1, 2]. Compared with other wide band gap semiconductor materials, such as diamond, GaN, SiC, ZnO, it has many advantages for device applications including lower growth temperature and higher radiation hardness, which are suitable for fabrication of long-lifetime devices. Owing to large exciton binding energy (60 mV), ZnO has attracted increasing attention that it can be integrated with photodetectors [3]. Additionally, it can be alloyed with MgO in order to tailor the band gap as demonstrated by Kawasaki *et al* [4] and Minemoto *et al* [5]. Due to the difficulty of the realization of p–n junction-based devices, metal–semiconductor–metal (MSM) structure UV photodetectors based on ZnO and $Mg_xZn_{1-x}O$ have been demonstrated in recent years [6–8].

$Mg_xZn_{1-x}O$ exists in the form of hexagonal and rock-salt structures corresponding to Mg composition in ZnO. By varying the Mg composition, the band gap can be tuned from 3.3 to 7.8 eV. Due to this advantage, $Mg_xZn_{1-x}O$ UV detectors have significant commercial and scientific potential application value for engine control, solar UV monitoring, astronomy, space-to-space communications and detection of missile plumes, located in the UV-B region. At present, most reports about the Mg composition in the $Mg_xZn_{1-x}O$ film show that it is usually less than 33% of UV detectors. That is because high Mg composition will produce phase splitting due to the different structures of ZnO and MgO. Furthermore, $Mg_xZn_{1-x}O$ UV detectors are of photoconductive type [8, 9], which primarily have a long response time and large dark current defects. In this paper, a high-speed photoconductive UV detector based on the $Mg_{0.4}Zn_{0.6}O$ film with the MSM structure was obtained, and the factors which affected the response speed of the device have been analysed.

2. Experiments

An $Mg_{0.4}Zn_{0.6}O$ thin film on a quartz substrate was fabricated by the rf magnetron sputtering technique, which had a base pressure of 5.0×10^{-4} Pa. The $Mg_{0.18}Zn_{0.82}O$ target to quartz substrate distance was maintained at 6 cm and the substrate temperature was 673 K. The working pressure in the chamber was kept at 1 Pa during the film growth. The rf power was kept at 100 W and the applied voltage was 500 V. Ultrapure (5 N) Ar and N_2 gases were introduced into the sputtering chamber through a set of mass flow controllers with flow rates of 22.5 sccm (standard cubic centimetre per minute). The rate of deposition was adjusted so as

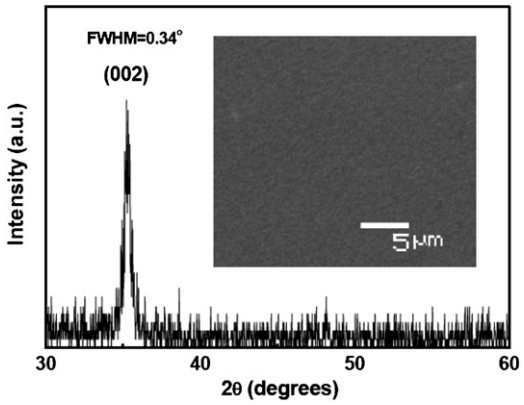

Figure 1. XRD pattern of the $Mg_{0.4}Zn_{0.6}O$ film deposited on a quartz substrate. Inset: the SEM photograph of the $Mg_{0.4}Zn_{0.6}O$ film.

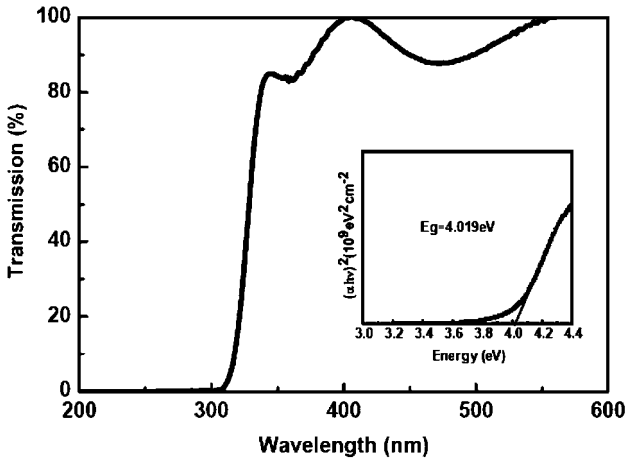

Figure 2. Transmission spectra of the $Mg_{0.4}Zn_{0.6}O$ film. The inset shows $(\alpha h\nu)^2$ versus $h\nu$ that gives the room temperature band gap.

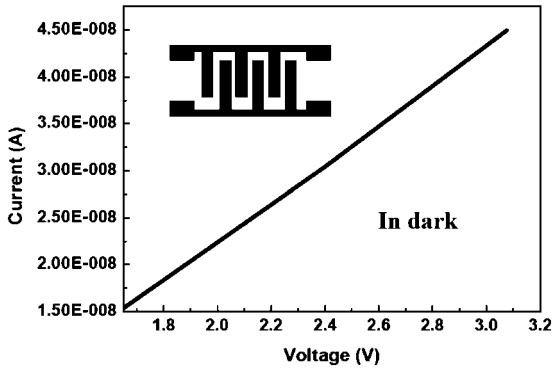

Figure 3. Current–voltage characteristics of Au–Zn contacts in the dark. A schematic view of the interdigitated configuration of the device is shown in the inset.

to have a film thickness of nearly 500 nm (measured by scanning electron micrograph (SEM)) for a film growth for 60 min. Following, the $Mg_xZn_{1-x}O$ thin film was annealed at 673 K in vacuum about 5.0×10^{-4} Pa for 30 min. Then, the high resistance ($\sim 10^7\ \Omega$) $Mg_xZn_{1-x}O$ thin film was obtained. The MSM structure with interdigitated configuration on the $Mg_{0.4}Zn_{0.6}O$ film was obtained by lithography and wet etching. It consists of 12 fingers at each electrode finger, which are 5 μm wide, 500 μm long and have a pitch of 2 μm.

The structure characterization of the alloy thin film was carried out by x-ray diffraction (XRD) using a D/max-RA x-ray spectrometer (Rigaku) with Cu Kα radiation of 0.154 nm. A Hitachi S4800 SEM was employed to study the surface morphology of the film. Energy dispersive spectroscopy (EDS) was used to determine the Mg/Zn ratio in the film. The acceleration voltage and the magnification of EDS were 10 kV and 5000, respectively. Optical transmission spectra were recorded using a Shimadzu UV-3101 PC scanning spectrophotometer.

For the characterization of the $Mg_{0.4}Zn_{0.6}O$ UV detectors, a pulsed Nd-YAG laser (266 nm, 10 ns) and a 150 W Xe lamp were used as the excitation source. The spectrum response was measured by a lock-in amplifier. The dark current was measured by the Hall measurement system.

3. Results and discussion

The crystal structure of the annealed film was shown by XRD measurement. As shown in figure 1, the peak at $2\theta = 35.283^\circ$ corresponds to (0 0 2) orientation of the single wurtzite structure with the c-axis lattice parameter of 0.508 nm, which is close to the ZnO c-axis lattice constant. No signatures of the cubic phase (peak at $2\theta = 36.70^\circ$ for (1 1 1) orientation) were observed. The Mg composition in the film was measured by EDS and obtained to be $Mg_{0.4}Zn_{0.6}O$. No other impurities were detected within the detection limit of EDS ($\sim$0.5 wt%). With the higher thermodynamic solubility of Mg in ZnO (up to 40%), the alloy film remained in a single phase and was in close agreement with the observations of Kumar *et al*, who reported a solubility limit of 42% for $Mg_xZn_{1-x}O$ films prepared by the same technique at room temperature [10]. The difference between the Mg percentage in the target and in the film was attributed to the high vapour pressure of Zn, resulting in high Mg composition in the film with a larger band gap. The inset in figure 1 shows the SEM images of the $Mg_{0.4}Zn_{0.6}O$ film. It has moderately smooth surface morphology. It is believed that the formation of the uniform interface between Au and ZnO conjunction.

Figure 2 presents the optical transmission in the wavelength range from 200 to 600 nm. From figure 2, it is observed that the transmittance varies significantly with the wavelength of 320 nm. The average transmittance in the visible part of the spectra was more than 85% after 340 nm. The band gap energy was derived from the line shown in the inset of figure 2. The optical band gap of $Mg_{0.4}Zn_{0.6}O$ was about 4.2 eV [11]. A similar result has been reported by Minemoto *et al* who obtained a stable $Mg_xZn_{1-x}O$ alloy up to the solubility limit of 46% [12]. From the inset, we can see that the tail and bow of the absorption edge are shown, which would be attributed to the structural defects; for example, Mg may be incorporated at the interstitial sites and grain boundaries.

The $Mg_{0.4}Zn_{0.6}O$ MSM structure with interdigitated configuration was used to evaluate the UV detector performance. The measured dark I–V characteristics are shown in figure 3. The linear I–V relations under both forward and reverse biases exhibit ohmic metal–semiconductor contacts. Under 3 V bias, the dark current was no more than 40 nA. The low dark current is helpful to enhance

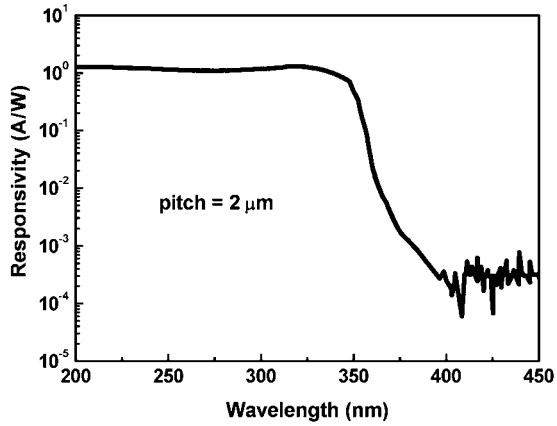

Figure 4. Spectral response of the $Mg_{0.4}Zn_{0.6}O$ UV detector.

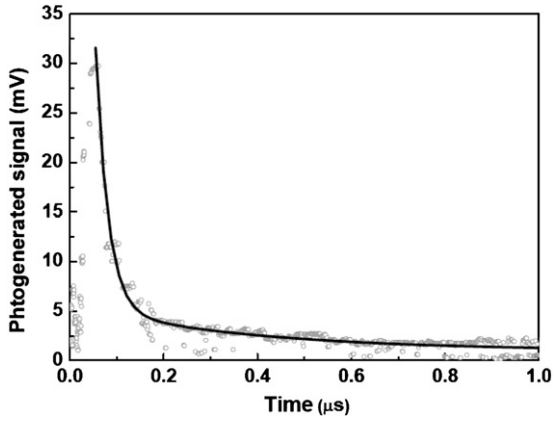

Figure 5. Response time of the $Mg_{0.4}Zn_{0.6}O$ UV detector with a load resistance of 50 Ω.

the detector's signal-to-noise (S/N) ratio since the shot noise, which exceeds the Johnson and $1/f$ noise if the operating frequency is not too low, is proportional to the dark current [8]. Hence, the low dark current, in our case, contributes to the high quality $Mg_{0.4}Zn_{0.6}O$ film.

Figure 4 shows the spectral response of the $Mg_{0.4}Zn_{0.6}O$ MSM UV detector. The responsivity is quite flat over the band gap, and the responsivity of the detector was about 1.3 A W^{-1} at 320 nm under 3 V bias. The UV-to-visible rejection was more than four orders of magnitude from 320 to 400 nm. Furthermore, it was hard to detect any photogenerated signal for wavelengths longer than 420 nm ($R < 10^{-5}$ A W^{-1}). The maximum responsivity corresponds to the external quantum efficiency of 505%. The noise equivalent power (NEP) can be calculated by NEP $= (4k_BT/R_{dark} + 2qI_{dark})^{1/2}\Delta f^{1/2}/R$, where R_{dark} refers to the equivalent resistance obtained from the slope of the dark current I–V curve at the bias point, I_{dark} is the dark current at the bias point, T is the temperature, Δf is the bandwidth of the measurement and R is the measured responsivity. The normalized detectivity (D^*) can then be determined by $D^* = (A\Delta f)^{1/2}/\text{NEP}$, where A is the device area. With a 3 V applied bias, it was found that we achieved the maximum D^* of 1.37×10^{11} cm $Hz^{1/2}$ W^{-1} at 320 nm. It should be noted that D^* measured from our $Mg_{0.4}Zn_{0.6}O$ UV detector was higher than those observed from GaN-based MSM photodetectors with a similar structure [13].

The time response was measured at 3 V bias with a load resistance of 50 Ω in figure 5. The inset is the enlarged impulse response. For the interdigitated spacing of 2 μm, the 10%–90% rise time and fall time were 16 ns and 250 ns, respectively. 80 ns was the full-width at half-maximum (FWHM) value of the time response. The 16 ns rise time was limited by the excitation laser, which has a nominal pulse duration FWHM of 10 ns. Hence, as shown in figure 5, no persistent photoconductivity was observed. Yang has fabricated a UV detector based on the $Mg_{0.34}Zn_{0.66}O$ thin film grown by PLD. The rise time and fall time of the MSM photoconductivity detector were 8 ns and 1.4 μs, respectively [8]. To the best of our knowledge, this is the fastest reported $Mg_{0.40}Zn_{0.60}O$ photoconductive UV detector. It is obvious that our detector had advantages in the fall time. This indicates that the $Mg_{0.40}Zn_{0.60}O$ thin film which we have prepared is of high quality, especially after annealing. However, the fall time was longer than the rise time. So it is necessary to consider various physical effects. The slower fall time can be very well fitted with a bi-exponential function with the time constants of 6.5 and 39.2 ns. They were attributed to the electron and the hole components, respectively.

The transit time and *RC* constant are related to the time response. t_τ is the transit time of the electrons between two electrodes [14]. $t_\tau = L^2/\mu_e V$, where L is the interdigitated spacing, μ_e is the electron mobility and V is the voltage drop between the two electrodes. L, μ_e and V are 2 μm, 6 cm^2 V s^{-1} (measured by the Hall measurement) and 3 V, respectively. So the transit time (∼3 ns) is ruled out, and it may contribute to the 20 ns rise time, but has a negligible effect on the fall time. The *RC* time constant is estimated about 10 ns ($C \sim 0.5$ pF, measured by actual capacitance–voltage measurement), where C is the sum of the detector internal capacitance and the load capacitance, R is the load resistance and the series resistance [15]. The *RC* constant may be one part of the fall time. This indicates that mechanisms other than *RC* and transit limitations are responsible for the fall time part of the high-speed response of the $Mg_{0.40}Zn_{0.60}O$ UV detector. We postulate that the long and bi-exponential fall times are mainly related to hole trapping at the semiconductor–metal interface in the $Mg_xZn_{1-x}O$ film [16], where photogenerated carriers can be trapped at these sites. The long decay tail is possibly formed by the arrival of such released carriers which are trapped in these sites for a rather long time. In addition, the oxygen adsorption at the surface of the $Mg_xZn_{1-x}O$ film may be another reason [17]. So there is a gain in the detector, and it performs a direct proportion with electron carrier lifetime and responsivity [18]. This can be explained by the effect of gain on the fall time and responsivity.

4. Conclusion

In summary, the high-speed photoconductive UV detector based on the high quality $Mg_{0.4}Zn_{0.6}O$ film had been fabricated and characterized. The fabricated devices exhibited low leakage with dark current less than 40 nA below 3 V bias. The maximal peak responsivity of 1.3 A W^{-1} at 320 nm was measured at 3 V bias, corresponding to an external

quantum efficiency of 505% and the detectivity D^* of 1.37 $\times$ 10^{11} cm $Hz^{1/2}$ W^{-1}. An ultraviolet-rejection ratio (320 nm/400 nm) of more than four orders of magnitude was obtained from the fabricated detector. The 10%–90% rise and fall times were 16 ns and 250 ns, respectively. We deem that the slow response in the $Mg_{0.4}Zn_{0.6}O$ UV detector is usually attributed to the hole trapping at the semiconductor–metal interface and the oxygen adsorption at the surface. We deeply believe that if the quality of the $Mg_xZn_{1-x}O$ film is enhanced, the response time will be faster.

Acknowledgments

This work is supported by the key project of National Natural Science Foundation of China under grant nos 60336020, 50532050, the Innovation Project of Chinese Academy of Sciences, and the National Natural Science Foundation of China under grant nos 60429403, 10674133 and 60506014.

References

[1] Barnes T M, Leaf J, Hand S, Fry C and Wolden C A 2004 A comparison of plasma-activated N_2/O_2 and N_2O/O_2 mixtures for use in ZnO:N synthesis by chemical vapor deposition *J. Appl. Phys.* **96** 7036–44

[2] Kato H, Sano M, Miyanoto K and Yao T 2003 Homoepitaxial growth of high-quality Zn-polar ZnO films by plasma-assisted molecular beam epitaxy *Japan. J. Appl. Phys.* **42** L1002–5

[3] Look D C, Reynolds D C, Hemsky J W, Jomes R L and Sizelove J R 1999 Production and annealing of electron irradiation damage in ZnO *Appl. Phys. Lett.* **75** 811–3

[4] Ohtomo A, Kawasaki M, Koida T, Masubuchi K, Koinuma H, Sakurai Y, Yoshida Y, Yasuda T and Segawa Y 1998 Mg_xZn_{1-x} as a II–VI widegap semiconductor alloy *Appl. Phys. Lett.* **72** 2466–8

[5] Minemoto T, Negami T, Nishiwaki S, Takakura H and Hamakawa Y 2000 Preparation of $Zn_{1-x}Mg_xO$ films by radio frequency magnetron sputtering *Thin Solid Film* **372** 173–6

[6] Liang S, Sheng H, Liu Y, Huo Z, Lu Y and Shen H 2001 ZnO Schottky ultraviolet photodetectors *J. Cryst. Growth* **225** 110–3

[7] Xu Q A, Zhang J W, Ju K R, Yang X D and Hou X 2006 ZnO thin film photoconductive ultraviolet detector with fast photoresponse *J. Cryst. Growth* **289** 44–7

[8] Yang W, Vispute R D, Choopun S, Sharma R P, Venkatesan T and Shen H 2001 Ultraviolet photoconductive detector based on epitaxial $Mg_{0.34}Zn_{0.66}O$ thin films *Appl. Phys. Lett.* **78** 2787–9

[9] Yang W, Hullavarad S S, Nagaraj B, Takeuchi I, Sharma R P, Venkatesan T, Vispute R D and Shen H 2003 Compositionally-tuned epitaxial cubic Mg_xZn_{1-x} on Si(1 0 0) for deep ultraviolet photodetectors *Appl. Phys. Lett.* **82** 3424–6

[10] Kumar S, Gupte V and Sreenivas K 2006 Structural and optical properties of magnetron sputtered $Mg_xZn_{1-}O$ thin films *J. Phys: Condens. Matter* **18** 3343–54

[11] Pawlikowski J M 1982 Absorption edge of Zn_3P_2 *Phys. Rev.* B **26** 4711–3

[12] Minemoto T, Negami T, Nishiwaki S, Takakura H and Hamakawa Y 2000 Preparation of $Zn_{1-x}Mg_xO$ films by radio frequency magnetron sputtering *Thin Solid Films* **372** 173–6

[13] Wang C K, Chang S J, Su Y K, Chiou Y Z, Chang C S, Lin T K, Liu H L and Tang J J 2005 High detectivity GaN metal–semiconductor–metal UV photodetectors with transparent tungsten electrodes *Semicond. Sci. Technol.* **20** 485–9

[14] Basak D, Amin G, Mallik B, Paul G K and Sen S K 2003 Photoconductive UV detectors on sol–gel-synthesized ZnO films *J. Cryst. Growth* **256** 73–7

[15] Monroy E, Palacios T, Hainaut O, Omnes F and Calle F 2002 Assessment of GaN metal–semiconductor–metal photodiodes for high-energy ultraviolet photodetection *Appl. Phys. Lett.* **80** 3198–20

[16] Katz O, Bahir G and Salzman J 2004 Persistent photocurrent and surface trapping in GaN Schottky ultraviolet detectors *Appl. Phys. Lett.* **84** 4092–4

[17] Zhang D H 1996 Adsorption and photodesorption of oxygen on the surface and crystallite interfaces of sputtered ZnO films *Mater. Chem. Phys.* **45** 248–52

[18] Zhao Z M, Jiang R L, Chen P, Xi D J, Luo Z Y, Zhang R, Shen B and Chen Z Z 2000 Metal–semiconductor–metal GaN ultraviolet photodetectors on Si(1 1 1) *Appl. Phys. Lett.* **77** 444–6